

MoVi: A Large Multipurpose Motion and Video Dataset

Saeed Ghorbani
York University
Toronto, ON, Canada
saeed@eecs.yorku.ca

Kimia Mahdavian
Queen's University
Kingston, ON, Canada

Anne Thaler
York University
Toronto, ON, Canada

Konrad Kording
University of Pennsylvania
Philadelphia, USA

Douglas James Cook
Queen's University
Kingston, ON, Canada

Gunnar Blohm
Queen's University
Kingston, ON, Canada

Nikolaus F. Troje
York University
Toronto, ON, Canada

Abstract

Human movements are both an area of intense study and the basis of many applications such as character animation. For many applications it is crucial to identify movements from videos or analyze datasets of movements. Here we introduce a new human Motion and Video dataset MoVi, which we make available publicly. It contains 60 female and 30 male actors performing a collection of 20 predefined everyday actions and sports movements, and one self-chosen movement. In five capture rounds, the same actors and movements were recorded using different hardware systems, including an optical motion capture system, video cameras, and inertial measurement units (IMU). For some of the capture rounds the actors were recorded when wearing natural clothing, for the other rounds they wore minimal clothing. In total, our dataset contains 9 hours of motion capture data, 17 hours of video data from 4 different points of view (including one hand-held camera), and 6.6 hours of IMU data. In this paper, we describe how the dataset was collected and post-processed; We present state-of-the-art estimates of skeletal motions and full-body shape deformations associated with skeletal motion. We discuss examples for potential studies this dataset could enable.

Keywords

Human motion dataset, optical motion capture, IMU, video capture

1. Introduction

Recent advances in computer vision, in particular deep learning systems, have generated much interest in 2D human pose estimation [9, 55, 45, 14, 20, 26, 54, 51, 53, 29], 3D pose estimation [37, 43, 57, 47, 38, 52, 11, 39, 3, 41], human motion modelling [36, 17, 27, 23, 44, 22, 42, 19, 24, 4], 3D body reconstruction [30, 41, 40, 28], and activity recognition [50, 16, 60, 10, 58, 48, 7, 59, 31, 13, 15] that are based on video data. Large high-quality datasets are the cornerstone of such data-driven approaches.

While there are many publicly available datasets of human motion recordings [49, 35, 12, 56, 25], they are limited in that they either contain data of a small number of different actors, use single hardware systems for motion recording, or provide unsynchronized data across different hardware systems. We overcome these limitations with our large Motion and Video dataset (MoVi) that contains five different subsets of synchronised and calibrated video, optical motion capture (MoCap), and inertial measurement units (IMU) data of 90 female and male actors performing a set of 20 predefined everyday actions and sports movements, and one self-chosen movement. MoVi is a multi-purpose human video and motion dataset designed for a variety of challenges such as human pose estimation, action recognition, motion modelling, gait analysis, and body shape reconstruction. To our knowledge, this is one of the largest datasets in terms of the recorded number of actors and performed actions.

The 3D ground truth skeletal pose in MoVi was computed using two different pipelines: V3D (bio-mechanics formulation) [1] and MoSh++ (regression model) [34]. This allows a comparison of these two formulations and pro-

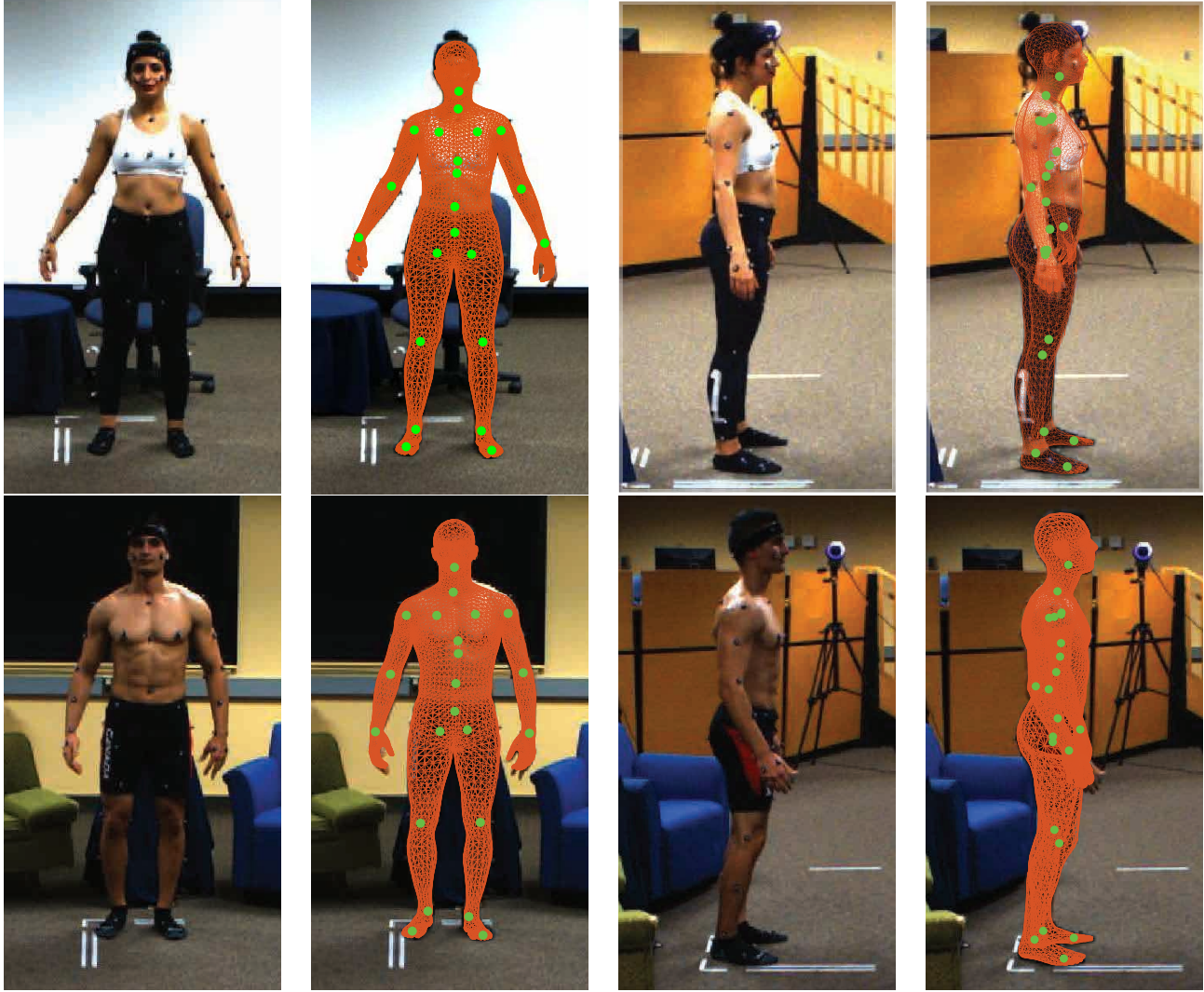


Figure 1: Front and side view of aligned video frame, joint locations, and estimated body mesh (computed by MoSh++) for one female and male actor.

vides more options for the computed pose, depending on the tasks and challenges at hand (see section 2.5). MoVi is also part of the Archive of Motion Capture as Surface Shapes (AMASS) [34], available at <https://amass.is.tue.mpg.de/>. The approach of AMASS allows to estimate accurate body shape that is factorized into individual, pose-independent shape components and pose-dependent components for every single frame of the MoCap recordings. The resulting animated 3D meshes can be aligned with the camera coordinate system and be treated as ground truth 3D body shapes (Figure 1).

2. The MoVi Dataset

2.1. Summary of the Data

MoVi contains data from 90 subjects performing the same predefined set of 20 actions and one self-chosen movement in five rounds of data capturing. 90 people (60 females, 30 males; 5 left handed) were recruited from the local Kingston community. Descriptive statistics of all participants are shown in Table 1. Participants provided written informed consent. The experimental procedure was approved by the ethics committee of Queen’s University, Kingston, and was performed in accordance with the Declaration of Helsinki.

The actors performed the same predefined set of 20 movements in a randomised order in five data capturing se-

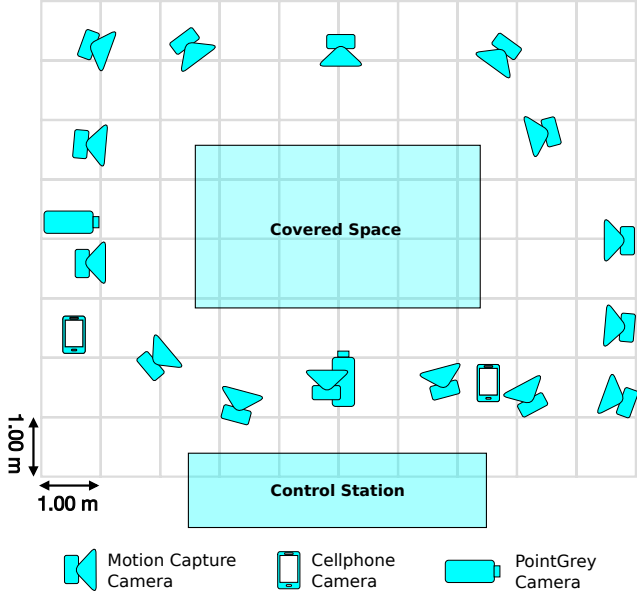


Figure 2: Top view sketch of the capture room set-up. The position of the video cameras and motion capture cameras were arranged to cover a space of approximately 3 by 5 meters.

	Females	Males
Height (m)	1.65 (0.08)	1.75 (0.06)
Weight (kg)	60.35 (8.03)	72.3 (10.98)
BMI (kg/m ²)	22.16 (3.02)	23.6 (3.24)
Age (y)	20.47 (3.59)	23.6 (3.61)

Table 1: Descriptive statistics (Mean (SD)) of the 60 female and 30 male actors.

quences. The movements included everyday actions and sports movements: (1) Walking, (2) Jogging, (3) Running in place, (4) Side gallop, (5) Crawling, (6) Vertical jumping, (7) Jumping jacks, (8) Kicking, (9) Stretching, (10) Cross arms, (11) Sitting down on a chair, (11) Crossing legs while sitting, (13) Pointing, (14) Clapping hands, (15) Scratching one’s head, (16) Throwing and catching, (17) Waving, (18) Pretending to take a picture, (19) Pretending to talk on the phone, (20) Pretending to check one’s watch. In each of the five sequences, the actors additionally performed one self-chosen motion (21).

The five sequences of data capturing differed in the hardware systems used to capture the motions, in participants’ clothing (minimal, or normal), and whether or not there was a rest pose between successive motions. An overview of the different capture rounds is provided in Table 2, technical

details of the hardware systems are provided in Table 3.

Data capture sequence “*F*” was captured using the 67 MoCap marker layout suggested in MoSh [32]. Actors wore tight-fitting minimal clothing in order to minimize marker movement relative to the body. The markers were attached onto the actors’ skin and clothes using double-sided tape. The MoCap system was synchronized with two video cameras capturing the actions from different viewpoints (front and side). Those two cameras were calibrated by computing the translation and rotation of the cameras relative to the coordinate system of the MoCap system. Two hand-held cellphone cameras were additionally used, however, the recordings were neither synchronized nor calibrated against the MoCap system. The different actions were separated by a rest A-pose. In our dataset, we provide the unedited full sequence of all motions, as well as trimmed MoCap and video sequences of the single motions. Our motivation for this capture round was to obtain accurate full skeletal (pose) information and frame-by-frame body shape parameters without any artifacts imposed by clothing. Therefore, this round can be considered more suitable for 2D or 3D pose estimation and tracking, and 3D shape reconstruction. The data collected in “*F*” was processed using two different pipelines: MoSh++ [34] and V3D [1] (see 2.5). Example images of a female and male actor in rest pose are shown in Figure 1.

To achieve more natural looking capture data, we recorded four more capture rounds where the actors wore normal clothing. Data capture rounds “*S1*” and “*S2*” were captured with a sparse set of 12 MoCap markers (4 markers placed on the head, 2 on each ankle and 2 on each wrist) which allowed the participants to wear normal clothing. Having the attached markers we could accurately extract the main end-effectors including the head, wrists, and ankles. It further allowed us to synchronize the IMU data with the MoCap and video capture system (Section 2.3). The actions were additionally recorded using synchronized computer vision cameras, cellphone cameras, and an IMU system. Whereas a rest A-pose separated the actions in “*S1*”, there was a natural transition between the different actions in “*S2*”. This setup was used as it allows to infer the pose and body shape by fusing a sparse marker set and IMU recordings while keeping the clothing natural.

While real clothing is essential for many meaningful data, it precludes the use of certain motion capture techniques. The data capture rounds “*I1*” and “*I2*” were thus captured using only IMU and video cameras (not synchronised). Motions in “*I1*” are separated by a rest A-pose, whereas there is a natural transition between the different actions in “*I2*”. The data collected in “*I1*” and “*I2*” is suitable for researchers that aim for computing pose or body shape without any artifacts imposed by the optical markers. The examples of the IMU suit used for “*S1*”, “*S2*”,

“I1”, and “I2” are shown in Figure 3. These recordings thus promise to enable a broad range of real-world applications.

2.2. Hardware

The movements were captured using two different hardware systems, an optical motion capture system and an inertial measurement unit system. We used a commercial optical motion capture system from Qualisys with fifteen 1.3 MP cameras that provide the 3D location of passive reflective markers with a frame rate of 120 per second. For the IMU system, we used the Noiton Neuron Edition V2 which comes as a suit attached with 18 IMU sensor. Each sensor is composed of a 3-axis gyroscope, a 3-axis accelerometer, and a 3-axis magnetometer working with 120 fps. In addition to the global acceleration data, the IMU suit provides 3D displacements, speed, quaternions, and rotational speed for each joint. For distinct questions different hardware will be useful. For example, IMUs are great at acceleration, while other capture systems produce high precision. The use of different, complementary hardware system promises to allow a broad range of meaningful analyses.

Video data was collected using two different types of cameras, smartphone cameras and computer vision cameras. We used two hand-held iPhone 7 smartphone cameras with a 800×600 resolution, global shutter, and 30 fps. As opposed to the computer vision cameras, the footage obtained with those smartphone cameras is shaky due to natural arm and hand movements. The video quality is similar to what the majority of commercially available smartphone cameras provides to date. For the two computer vision cameras we used Grasshoppers cameras from FLIR Inc company with 800×600 Sony ICX285 CCD sensors. The recordings of the FLIR cameras are synchronized with the MoCap cameras with 30 fps (aligned with every fourth frame of the MoCap system). Detailed information of the used hardware is provided in Table 3. Figure 2 shows the top-view floor plan and the location of the MoCap and video cameras. The process of how the devices were synchronized are described in Section 2.3, the camera calibration is describes in Section 2.4.

2.3. Synchronization

MoCap and Video

To provide a frame-by-frame accurate 3D motion overlaid on the video footage, the motion capture system should be synchronized with cameras in frame and then calibrated to the same coordinate. The synchronization between motion capture cameras and the FLIR Grasshoppers video cameras was done in hardware. In our setup, the video cameras were triggered by the synchronization signal provided by the MoCap system. Due to the frame rate limits in video

cameras, the synchronization frequency was divided by 4 which reduced the video capture frame rate to 30 fps. The phone cameras were not synchronized with the motion capture cameras.

IMU

In round “S1” and “S2”, we used a reduced optical motion marker set layout with 12 markers. Although the main motivation for using this reduced marker set was to allow the actors to wear natural clothing, this small set of markers offers several advantages: 1) It provides sparse but accurate data for some of the main joints (head, wrists, and ankles). The data can be applied in a data fusion approach along with IMU data to infer the exact joint locations. We leave this to future work. 2) It allowed us to synchronized IMU and MoCap data. To synchronize the data, we used cross-correlation between these two modalities. The two coordinate systems were not aligned, however, the differences between the orientation of the two z axes is negligible: the z axis of the IMU coordinate system is oriented towards gravity, while z axis in MoCap coordinate system is perpendicular to the floor. Because the MoCap system was synchronised with the video cameras (Section 2.3), we additionally obtained synchronized IMU and video data.

Suppose $v_z^j(t)$ and $\tilde{v}_z^j(t)$ are the z component of tracked position of joint j recovered by the motion capture and IMU systems, respectively (we are using the 3D positions provided by the IMU software instead of double-integrating over accelerations). The synchronization parameters, temporal scale α and temporal shift β , are found by maximizing:

$$\max_{\alpha, \beta} \max_{\tau} (v_z^j(t) \star \tilde{v}_z^j(\alpha t + \beta))(\tau), \quad (1)$$

where

$$(v_z^j(t) \star \tilde{v}_z^j(\alpha t + \beta))(\tau) \triangleq \int_{-\infty}^{\infty} v_z^j(t) \tilde{v}_z^j(\alpha t + \beta + \tau) dt, \quad (2)$$

is the cross-correlation between $v_z^j(t)$ and shifted-and-scaled version of $\tilde{v}_z^j(t)$. α and β are the scale and shift parameters, respectively. The optimal parameters are those which achieve the highest peak in cross-correlation.

The procedure mentioned above was done for left and right ankles and checked qualitatively for all data.

2.4. Calibration

The calibration of the MoCap cameras were done by a measurement procedure in Qualisys Track Manager software [46]. The software allows to compute the orientation and position of each camera in order to track and perform calculations on the 2D data into 3D data. To compute the



Figure 3: Example pictures of one female and one male actor wearing the IMU suits used for the capture rounds S1, S2, I1, and I2.

Round	F	S1	S2	I1	I2
MoCap marker set	67	12	12	–	–
Video capture	yes	yes	yes	yes	yes
IMU	no	yes	yes	yes	yes
A-pose between motions	yes	yes	no	yes	no
Actor clothing	minimal	normal clothing	normal clothing	normal clothing	normal clothing
Length (min per person)	~ 2.7	~ 2.7	~ 1.7	~ 2.7	~ 1.7

Table 2: Overview of the five difference capture rounds. F = Full; S = sparse marker set + IMU; I = IMU.

computer vision cameras’ intrinsics and lens distortion parameters, we used the MATLAB Single Camera Calibrator [21, 61, 8], where focal length ($F \in \mathbb{R}^2$), optical center ($C \in \mathbb{R}^2$), skew coefficient ($S \in \mathbb{R}$), and radial distortion ($D \in \mathbb{R}^2$) are estimated for each camera.

The extrinsic parameters which represent the rotation $R \in SO(3)$ and translation $T \in \mathbb{R}^3$ transformations from world coordinates (MoCap coordinate system) to camera coordinates, are estimated using the semi-automated method proposed by Sigal et al. [49]. The trajectory of a single moving marker was recorded by synchronized MoCap and video cameras for around 2000 synchronized frames. Given the recorded 3D positions of the marker in MoCap coordinates as world points and the 2D positions of the marker in the camera frame as image points, the problem of finding the best 2D projection can be formulated as a Perspective- n -Point (PnP) problem where the Perspective-Three-Point (P3P) algorithm [18] is used to minimize the re-projection error as follows:

$$\min_{R,T} \sum_{t=1}^N \|P_{2D} - f(P_{3D}; R, T, K)\|^2, \quad (3)$$

where f is the projection function and $K \in \{F, C, S, D\}$ is the set of camera intrinsics parameters.

2.5. Skeleton and Body Shape Extraction from Mo-Cap data

The skeleton (joint locations and bones) were computed with two different pipelines. Visual 3D software (manufacturer C-MOTION): Visual 3D is an advanced biomechanics analysis software for 3D motion capture data [1]. In our V3D pipeline, pelvic segment was created using CODA [2] and the hip joints positions were estimated by Bell and Brand hip joint center regression [5, 6]. The upper body parts were estimated using Golem/Plug-in Gait Upper Extremity model as implemented in Vicon [1]. The skeleton is represented by 20 joints in two different formats: 1) in

MoCap System	Brand and model	Qualisys Oqus 300 and 310
	Number of cameras	15
	Resolution	1.3 megapixel
	Frame rate	120 Hz
	Synchronized	Yes
Video Capture Systems 1	Brand and model	FLIR, Grasshopper
	Number of cameras	2
	Cameras synchronized	Yes
	Cameras calibrated	Yes
	Resolution	800 x 600 pixels, 72 dpi, 24 bit depth
	Sensor	Sony ICX285, CCD
	Frame rate	30 Hz
File type	JPEG frames and AVI video files	
Video Capture Systems 2	Brand and model	IPhone 7 rear camera
	Number of cameras	2
	Cameras synchronized	No
	Cameras calibrated	No
	Resolution	1920 x 1080 pixels
	Sensor	Sony Exmor RS, CMOS
	Frame rate	30 Hz
File type	MP4 video files	
IMU	Brand and model	Noitom, Neuron Edition V2
	Number of sensors	18 Neurons
	Sensor	9-axis IMU composed of 3-axis gyroscope, 3-axis accelerometer, and 3-axis magnetometer
	Synchronized	in S1 and S2 rounds
	Frame rate	120 Hz
File type	BVH and calculation files	

Table 3: Technical details of the hardware systems used to capture the MoVi dataset.

joint angles, that is the angle of each bone relative to coordinate system of its parent joint, and 2) as global 3D joint locations.

MoSh++: MoSh++[34] is an approach which estimates the body shape, pose, and soft tissue deformation directly from motion capture data. Body shape and pose are represented using a rigged body model called SMPL[33] where the pose is defined by joint angles and shape is specified by shape blend shapes. MoSh++ uses a generative inference approach whereby the SMPL body shape and pose parameters are optimized to minimize reconstruction errors. The skeletal Joints location are computed using a linear regression function of mesh vertices. The estimated SMPL body is extended by adding dynamic blend shapes using the dynamic shape space of DMPL. Each frame in the "MoShed" representation includes 16 SMPL shape coefficients, 8 DMPL dynamic soft-tissue coefficients, and 66 SMPL pose coefficients as joint angles (21 joints + 1 root). MoShed data was computed in collaboration with the authors of AMASS [34].

The main difference between the skeleton represented

by MoSh and the skeleton represented by V3D is that the MoShed version is generally more robust to occlusion because it uses distributed information, rather than doing the computations locally. This makes it a better choice for the task of pose estimation and tracking as the joints locations are all available over the time. However, the estimated joint location can be noisy during the occlusion and the error may propagate to other joints too. On the other hand, V3D provides a more accurate estimation of joint location. Therefore, one may prefer using the V3D joints representation for the task of gait analysis. The only drawback of V3D representation compared to MoSh++ is that the joints cannot be computed when a related marker is occluded.

Our dataset is the first sizable dataset including not only 3D joint locations, but also a highly accurate 3D mesh of the body which can be projected onto the video recordings. This can be useful for approaches that try to estimate body shape from video data.

<code>F_amass_subject_{<ID>.mat</code>	–	Contains the full marker set MoCap data processed by MoSh++ in the AMASS project and augmented with 3D joints’ positions and metadata. All files are compressed and stored as <code>F_AMASS.rar</code> . The original npz files and the rendered animation files are available at https://amass.is.tue.mpg.de/
<code><round>.v3d_subject_{<ID>.mat</code>	–	Contains the MoCap data processed by V3D and augmented with metadata. All files are compressed as <code>subject_1_45_F_V3D.rar</code> which contains “F” round data from subject 1 to 45, <code>subject_46_90_F_V3D.rar</code> which contains “F” round data from subject 46 to 90, and <code>S_V3D.rar</code> which contains “S1” and “S2” rounds data from all subjects.
<code>imu_subject_{<ID>.mat</code>	–	Contains the processed IMU calculation files augmented with metadata. Each file contains the data collected in all “S1”, “S2”, “I1”, “I2” rounds. All files are compressed as <code>IMU_calc.rar</code>
<code><round>.imu_subject_{<ID>.bvh</code>	–	Contains the bvh files generated by the IMU software. All files are compressed as <code>IMU_bvh.rar</code>
<code><round>_{<camera>}_subject_{<ID>.avi</code>	–	An AVI video data for each subject, round, and camera
<code>cameraParams_{<camera>.mat</code>	–	Contains the camera calibration data. Each file contains the MATLAB intrinsic camera parameter object
<code>Extrinsics_{<camera>.mat</code>	–	Contains the camera extrinsics parameters (rotation matrix and translation vector)

Table 4: MoVi dataset file structure. $\langle ID \rangle \in \{1, 2, \dots, 90\}$ is the subject number. $\langle round \rangle \in \{F, S1, S2, I1, I2\}$ is the data collection round (see Table 1). $\langle camera \rangle \in \{PG1, PG2, CP1, CP2\}$ is the camera type, where PG and CP indicate the computer vision and cellphone cameras, respectively

3. Dataset structure

We used the Dataverse repository to store the motion and video data. We provide the original AVI video files to avoid any artifacts added by compression methods. The processed MoCap data is provided in two different versions based on the post-processing pipeline (AMASS and V3D). We provide joint angles and joint 3D locations computed by both pipeline along with the associated kinematic tree, occlusions, and optical marker data. Synchronized IMU data (along with the original data) are computed by processing `calculation` files (see Section 2.3) and converted to `mat` format which provides raw acceleration data, displacement, velocity, quaternions and angular velocity. The `bvh` files generated by the IMU software are also provided on the website. The support code to use data in MATLAB and Python environments is also provided. The dataset naming structure is provided in Table 4.

4. Discussion and Conclusion

We provide the large Motion and Video dataset MoVi, which is now available at <https://www.biomotionlab.ca/movi>. The dataset contains motion recordings (optical motion capture, video, and IMU) of 90 male and female actors performing a set of 20 everyday actions and sports motions, and one additional self-chosen motion. The different sequences of the dataset contain synchronized recordings of the three different hardware systems. In addition, our full-body motion capture recordings are available as realistic 3D human meshed represented by a rigged body model as part of the AMASS dataset [34]. This allows video overlay of not only the body joints, but also the full body meshes. To our knowledge, MoVi is the first dataset with synchronized pose, pose-dependent shape, and video recordings. The multi-modality makes our dataset suitable for a wide range of challenges such as human pose estimation and tracking, body shape estimation, human motion prediction and synthesis, action recognition, and gait analysis.

Acknowledgments

We wish to thank Nima Ghorbani for post-processing our motion capture data so it could be added to the AMASS dataset (<https://amass.is.tue.mpg.de/>), and all others authors of AMASS for their approval to add the processed data to our dataset. We further wish to thank Viswajit Kumar for his help with post-processing the data and setting up the data repository and website. This research was funded by a NSERC Discovery Grant and contributions from CFREF VISTA to NFT.

References

- [1] C-motion research biomechanics. <http://www2.c-motion.com/index.php>.
- [2] Coda Pelvis visual3d wiki documentation. https://c-motion.com/v3dwiki/index.php?title=Coda_Pelvis. Accessed: 2019-11-07.
- [3] Rıza Alp Güler, Natalia Neverova, and Iasonas Kokkinos. Densepose: Dense human pose estimation in the wild. In *Proceedings of the IEEE Conference on Computer Vision and Pattern Recognition*, pages 7297–7306, 2018.
- [4] Emad Barsoum, John Kender, and Zicheng Liu. Hp-gan: Probabilistic 3d human motion prediction via gan. In *Proceedings of the IEEE Conference on Computer Vision and Pattern Recognition Workshops*, pages 1418–1427, 2018.
- [5] Alexander L Bell, Richard A Brand, and Douglas R Pedersen. Prediction of hip joint centre location from external landmarks. *Human movement science*, 8(1):3–16, 1989.
- [6] Alexander L Bell, Douglas R Pedersen, and Richard A Brand. A comparison of the accuracy of several hip center location prediction methods. *Journal of biomechanics*, 23(6):617–621, 1990.
- [7] Hakan Bilen, Basura Fernando, Efstratios Gavves, Andrea Vedaldi, and Stephen Gould. Dynamic image networks for action recognition. In *Proceedings of the IEEE Conference on Computer Vision and Pattern Recognition*, pages 3034–3042, 2016.
- [8] JY Bouguet. Camera calibration toolbox for matlab. http://www.vision.caltech.edu/bouguetj/calib_doc/. Accessed: 2019-11-07.
- [9] Zhe Cao, Gines Hidalgo, Tomas Simon, Shih-En Wei, and Yaser Sheikh. Openpose: realtime multi-person 2d pose estimation using part affinity fields. *arXiv preprint arXiv:1812.08008*, 2018.
- [10] Joao Carreira and Andrew Zisserman. Quo vadis, action recognition? a new model and the kinetics dataset. In *proceedings of the IEEE Conference on Computer Vision and Pattern Recognition*, pages 6299–6308, 2017.
- [11] Rishabh Dabral, Anurag Mundhada, Uday Kusupati, Safeer Afaque, Abhishek Sharma, and Arjun Jain. Learning 3d human pose from structure and motion. In *Proceedings of the European Conference on Computer Vision (ECCV)*, pages 668–683, 2018.
- [12] Fernando De la Torre, Jessica Hodgins, Javier Montano, Sergio Valcarcel, R Forcada, and J Macey. Guide to the carnegie mellon university multimodal activity (cmu-mmact) database. *Robotics Institute, Carnegie Mellon University*, 5, 2009.
- [13] Yong Du, Wei Wang, and Liang Wang. Hierarchical recurrent neural network for skeleton based action recognition. In *Proceedings of the IEEE conference on computer vision and pattern recognition*, pages 1110–1118, 2015.
- [14] Hao-Shu Fang, Shuqin Xie, Yu-Wing Tai, and Cewu Lu. Rmpe: Regional multi-person pose estimation. In *Proceedings of the IEEE International Conference on Computer Vision*, pages 2334–2343, 2017.
- [15] Christoph Feichtenhofer, Axel Pinz, and Richard Wildes. Spatiotemporal residual networks for video action recognition. In *Advances in neural information processing systems*, pages 3468–3476, 2016.
- [16] Christoph Feichtenhofer, Axel Pinz, and Andrew Zisserman. Convolutional two-stream network fusion for video action recognition. In *Proceedings of the IEEE conference on computer vision and pattern recognition*, pages 1933–1941, 2016.
- [17] Katerina Fragkiadaki, Sergey Levine, Panna Felsen, and Jitendra Malik. Recurrent network models for human dynamics. In *Proceedings of the IEEE International Conference on Computer Vision*, pages 4346–4354, 2015.
- [18] Xiao-Shan Gao, Xiao-Rong Hou, Jianliang Tang, and Hang-Fei Cheng. Complete solution classification for the perspective-three-point problem. *IEEE transactions on pattern analysis and machine intelligence*, 25(8):930–943, 2003.
- [19] Partha Ghosh, Jie Song, Emre Aksan, and Otmar Hilliges. Learning human motion models for long-term predictions. In *2017 International Conference on 3D Vision (3DV)*, pages 458–466. IEEE, 2017.
- [20] Kaiming He, Georgia Gkioxari, Piotr Dollár, and Ross Girshick. Mask r-cnn. In *Proceedings of the IEEE international conference on computer vision*, pages 2961–2969, 2017.
- [21] Janne Heikkilä, Olli Silven, et al. A four-step camera calibration procedure with implicit image correction. In *cvpr*, volume 97, page 1106. Citeseer, 1997.
- [22] Daniel Holden, Taku Komura, and Jun Saito. Phase-functioned neural networks for character control. *ACM Transactions on Graphics (TOG)*, 36(4):42, 2017.
- [23] Daniel Holden, Jun Saito, and Taku Komura. A deep learning framework for character motion synthesis and editing. *ACM Transactions on Graphics (TOG)*, 35(4):138, 2016.
- [24] Yinghao Huang, Manuel Kaufmann, Emre Aksan, Michael J Black, Otmar Hilliges, and Gerard Pons-Moll. Deep inertial poser: learning to reconstruct human pose from sparse inertial measurements in real time. *ACM Transactions on Graphics (TOG)*, 37(6):185, 2019.
- [25] Catalin Ionescu, Dragos Papava, Vlad Olaru, and Cristian Sminchisescu. Human3.6m: Large scale datasets and predictive methods for 3d human sensing in natural environments. *IEEE transactions on pattern analysis and machine intelligence*, 36(7):1325–1339, 2013.
- [26] Arjun Jain, Jonathan Tompson, Mykhaylo Andriluka, Graham W Taylor, and Christoph Bregler. Learning human

- pose estimation features with convolutional networks. *arXiv preprint arXiv:1312.7302*, 2013.
- [27] Ashesh Jain, Amir R Zamir, Silvio Savarese, and Ashutosh Saxena. Structural-rnn: Deep learning on spatio-temporal graphs. In *Proceedings of the IEEE Conference on Computer Vision and Pattern Recognition*, pages 5308–5317, 2016.
- [28] Angjoo Kanazawa, Michael J Black, David W Jacobs, and Jitendra Malik. End-to-end recovery of human shape and pose. In *Proceedings of the IEEE Conference on Computer Vision and Pattern Recognition*, pages 7122–7131, 2018.
- [29] Lipeng Ke, Ming-Ching Chang, Honggang Qi, and Siwei Lyu. Multi-scale structure-aware network for human pose estimation. In *Proceedings of the European Conference on Computer Vision (ECCV)*, pages 713–728, 2018.
- [30] Nikos Kolotouros, Georgios Pavlakos, Michael J Black, and Kostas Daniilidis. Learning to reconstruct 3d human pose and shape via model-fitting in the loop. In *Proceedings of the IEEE International Conference on Computer Vision*, pages 2252–2261, 2019.
- [31] Ye Liu, Liqiang Nie, Li Liu, and David S Rosenblum. From action to activity: sensor-based activity recognition. *Neuro-computing*, 181:108–115, 2016.
- [32] Matthew Loper, Naureen Mahmood, and Michael J Black. Mosh: Motion and shape capture from sparse markers. *ACM Transactions on Graphics (TOG)*, 33(6):220, 2014.
- [33] Matthew Loper, Naureen Mahmood, Javier Romero, Gerard Pons-Moll, and Michael J Black. Smpl: A skinned multi-person linear model. *ACM transactions on graphics (TOG)*, 34(6):248, 2015.
- [34] Naureen Mahmood, Nima Ghorbani, Nikolaus F Troje, Gerard Pons-Moll, and Michael J Black. Amass: Archive of motion capture as surface shapes. *arXiv preprint arXiv:1904.03278*, 2019.
- [35] Christian Mandery, Ömer Terlemez, Martin Do, Nikolaus Vahrenkamp, and Tamim Asfour. The kit whole-body human motion database. In *2015 International Conference on Advanced Robotics (ICAR)*, pages 329–336. IEEE, 2015.
- [36] Julieta Martinez, Michael J Black, and Javier Romero. On human motion prediction using recurrent neural networks. In *Proceedings of the IEEE Conference on Computer Vision and Pattern Recognition*, pages 2891–2900, 2017.
- [37] Dushyant Mehta, Oleksandr Sotnychenko, Franziska Mueller, Weipeng Xu, Srinath Sridhar, Gerard Pons-Moll, and Christian Theobalt. Single-shot multi-person 3d pose estimation from monocular rgb. In *2018 International Conference on 3D Vision (3DV)*, pages 120–130. IEEE, 2018.
- [38] Natalia Neverova, Riza Alp Guler, and Iasonas Kokkinos. Dense pose transfer. In *Proceedings of the European Conference on Computer Vision (ECCV)*, pages 123–138, 2018.
- [39] Mohamed Omran, Christoph Lassner, Gerard Pons-Moll, Peter Gehler, and Bernt Schiele. Neural body fitting: Unifying deep learning and model based human pose and shape estimation. In *2018 International Conference on 3D Vision (3DV)*, pages 484–494. IEEE, 2018.
- [40] Georgios Pavlakos, Vasileios Choutas, Nima Ghorbani, Timo Bolkart, Ahmed AA Osman, Dimitrios Tzionas, and Michael J Black. Expressive body capture: 3d hands, face, and body from a single image. In *Proceedings of the IEEE Conference on Computer Vision and Pattern Recognition*, pages 10975–10985, 2019.
- [41] Georgios Pavlakos, Luyang Zhu, Xiaowei Zhou, and Kostas Daniilidis. Learning to estimate 3d human pose and shape from a single color image. In *Proceedings of the IEEE Conference on Computer Vision and Pattern Recognition*, pages 459–468, 2018.
- [42] Dario Pavllo, Christoph Feichtenhofer, Michael Auli, and David Grangier. Modeling human motion with quaternion-based neural networks. *arXiv preprint arXiv:1901.07677*, 2019.
- [43] Dario Pavllo, Christoph Feichtenhofer, David Grangier, and Michael Auli. 3d human pose estimation in video with temporal convolutions and semi-supervised training. In *Proceedings of the IEEE Conference on Computer Vision and Pattern Recognition*, pages 7753–7762, 2019.
- [44] Dario Pavllo, David Grangier, and Michael Auli. Quaternet: A quaternion-based recurrent model for human motion. *arXiv preprint arXiv:1805.06485*, 2018.
- [45] Leonid Pishchulin, Eldar Insafutdinov, Siyu Tang, Bjoern Andres, Mykhaylo Andriluka, Peter V Gehler, and Bernt Schiele. Deepcut: Joint subset partition and labeling for multi person pose estimation. In *Proceedings of the IEEE Conference on Computer Vision and Pattern Recognition*, pages 4929–4937, 2016.
- [46] AB Qualisys. Qualisys track manager user manual. *Gothenburg: Qualisys AB*, 2006.
- [47] Helge Rhodin, Mathieu Salzmann, and Pascal Fua. Unsupervised geometry-aware representation for 3d human pose estimation. In *Proceedings of the European Conference on Computer Vision (ECCV)*, pages 750–767, 2018.
- [48] Shikhar Sharma, Ryan Kiros, and Ruslan Salakhutdinov. Action recognition using visual attention. *arXiv preprint arXiv:1511.04119*, 2015.
- [49] Leonid Sigal, Alexandru O Balan, and Michael J Black. Humaneva: Synchronized video and motion capture dataset and baseline algorithm for evaluation of articulated human motion. *International journal of computer vision*, 87(1-2):4, 2010.
- [50] Karen Simonyan and Andrew Zisserman. Two-stream convolutional networks for action recognition in videos. In *Advances in neural information processing systems*, pages 568–576, 2014.
- [51] Ke Sun, Bin Xiao, Dong Liu, and Jingdong Wang. Deep high-resolution representation learning for human pose estimation. *arXiv preprint arXiv:1902.09212*, 2019.
- [52] Xiao Sun, Bin Xiao, Fangyin Wei, Shuang Liang, and Yichen Wei. Integral human pose regression. In *Proceedings of the European Conference on Computer Vision (ECCV)*, pages 529–545, 2018.
- [53] Wei Tang, Pei Yu, and Ying Wu. Deeply learned compositional models for human pose estimation. In *Proceedings of the European Conference on Computer Vision (ECCV)*, pages 190–206, 2018.
- [54] Jonathan J Tompson, Arjun Jain, Yann LeCun, and Christoph Breger. Joint training of a convolutional network and a

- graphical model for human pose estimation. In *Advances in neural information processing systems*, pages 1799–1807, 2014.
- [55] Alexander Toshev and Christian Szegedy. Deeppose: Human pose estimation via deep neural networks. In *Proceedings of the IEEE conference on computer vision and pattern recognition*, pages 1653–1660, 2014.
- [56] Matthew Trumble, Andrew Gilbert, Charles Malleson, Adrian Hilton, and John Collomosse. Total capture: 3d human pose estimation fusing video and inertial sensors. In *BMVC*, volume 2, page 3, 2017.
- [57] Gul Varol, Duygu Ceylan, Bryan Russell, Jimei Yang, Ersin Yumer, Ivan Laptev, and Cordelia Schmid. Bodynet: Volumetric inference of 3d human body shapes. In *Proceedings of the European Conference on Computer Vision (ECCV)*, pages 20–36, 2018.
- [58] Gül Varol, Ivan Laptev, and Cordelia Schmid. Long-term temporal convolutions for action recognition. *IEEE transactions on pattern analysis and machine intelligence*, 40(6):1510–1517, 2017.
- [59] Limin Wang, Yu Qiao, and Xiaoou Tang. Action recognition with trajectory-pooled deep-convolutional descriptors. In *Proceedings of the IEEE conference on computer vision and pattern recognition*, pages 4305–4314, 2015.
- [60] Limin Wang, Yuanjun Xiong, Zhe Wang, Yu Qiao, Dahua Lin, Xiaoou Tang, and Luc Van Gool. Temporal segment networks: Towards good practices for deep action recognition. In *European conference on computer vision*, pages 20–36. Springer, 2016.
- [61] Zhengyou Zhang. A flexible new technique for camera calibration. *IEEE Transactions on pattern analysis and machine intelligence*, 22, 2000.